On the adjustment of the stress-based criterion in AS3600 for the requirement of confined boundary elements in reinforced concrete walls with low to moderate ductility

Mohammadmahdi Gharib[1], Amirhossein Hassanieh[2] and Michael King[3]

1. Corresponding Author. Senior Structural Analyst/Engineer, Taylor Thomson Whitting, 48 Chandos Street, St Leonards, NSW 2065, Australia. Email: mahdi.gharib@ttw.com.au

2. Senior Structural Analyst/Engineer, Taylor Thomson Whitting, 48 Chandos Street, St Leonards, NSW 2065, Australia. Email: amir.hassanieh@ttw.com.au

3. Associate Director, Taylor Thomson Whitting, 48 Chandos Street, St Leonards, NSW 2065, Australia. Email: michael.king@ttw.com.au

Abstract

The latest revision of the Australian concrete standard (AS3600-2018) has introduced considerable detailing requirements for the limited-ductile structural wall systems with an aim to improve their structural performance to an acceptable level in an ultimate seismic event. However, the new provisions for limited ductile walls were previously required only for wall systems with moderate ductility, and have significant design and construction implications. One of the major changes is the requirement of confined boundary elements with transverse reinforcement at discontinuous edges and around major openings of limited-ductile walls, in which were not required by AS3600-2009 and have not been clearly identified in research literature as being necessary. In this study, the suitability of the stress-based criterion in AS3600-2018 for determining if boundary elements are required, which currently has a single limit for both limited-ductile and moderately ductile structural walls, is evaluated in the context of Australian design practice. It is compared with a rational strain-based method and is shown to be conservative and inconsistent in terms of the expected level of ductility from these systems. An adjusted stress criterion is proposed, which depends on the expected level of ductility, wall geometry, and material properties.

Keywords: concrete wall, seismic, boundary element, confinement, ductility.

1. Introduction

The lateral load resisting system of the majority of low- to high-rise buildings in Australia generally consists of reinforced concrete walls, which are typically lightly reinforced and commonly designed with the assumption of limited/low ductility levels. The latest revision of the Australian concrete standard, i.e. AS3600-2018 (Standards Australia 2018), has introduced considerable new detailing requirements for limited ductile walls (LDW) (μ_Δ=2), primarily the requirement of boundary elements (BE), which were required in AS3600-2009 (Standards Australia 2009) in Appendix C only for moderately ductile structural walls (MDW) (μ_Δ=3). One of the main concerns is the stability of discontinuous edges at critical regions, which has been addressed by prescribing a maximum slenderness ratio for the wall, and introducing a stress-based criterion for the requirement of confined boundary elements with transverse reinforcement. The latter is defined as a critical limit for the extreme fibre compression stress from linear elastic analysis with gross cross-section properties, which is currently set to as a single limit (0.15f'$_c$) for both LDW and MDW. The method appears to be inspired by the conventional approach in ACI318 (American Concrete Institute 2019), which is applicable to special ductile walls (SDW) with even a less stringent (0.2f'$_c$) limit than in AS3600-2018. Despite its favourable features such as applicability and simplicity for designers, its reliability and conservatism had been argued in the literature (Wallace and Moehle 1992; Wallace and Orakcal 2002). This resulted in the introduction of more rational strain-based methods, which have been successfully incorporated into international design standards (American Concrete Institute 2019; British Standards 2004; Canadian Standards Association 2004; New Zealand Standard 2006).

In the context of the strain-based limits for the requirement of BE, the seminal work of Wallace et al. (Wallace 1995, 2012; Wallace and Orakcal 2002), defines the criterion as a maximum limit for the depth of the compression block at the ultimate limit state (ULS), depending on the target level of ultimate drift at the maximum considered earthquake (MCE). This method, with some simplifying assumptions, has been incorporated into ACI318 for SDW. The same concept has been incorporated into NZS3101 (New Zealand Standard 2006) by nominating the maximum limit for the depth of the neutral axis for different ductility classes. Eurocode 8 (British Standards 2004) also uses a strain-based approach and requires transverse reinforcement in compression regions where the compressive strain consistent with the curvature at ultimate drift exceeds a critical limit (0.0035). Despite the reliability of strain-based methods and their sound concept, their complexity may affect their utilisation by practitioners, especially in regions with low seismicity such as Australia. Therefore, the introduction of a reliable stress-based criterion, which is consistent with the strain-based approach and can be directly related to stress outputs from finite element (FE) simulations or hand calculations, holds significant merit for design purposes.

Australian research (Menegon 2018; Menegon et al. 2018) on the seismic performance of RC structural walls argues that satisfactory seismic performance for most LDW systems can be achieved through standard wall detailing without boundary elements, recommending only lapped U-bars at terminations of horizontal reinforcement. Therefore, it is valid to question the conservative introduction of a single-valued extreme fibre compression stress limit in AS3600-2018 for different ductility classes as the relevant stress state is reduced by the response modification factor. This results in more stringent requirements in LDW than what is required for

MDW and by ACI318 for SDW, which goes against the conceptual intent of ductility and is not rationally justified. In this study, an adjusted stress-based limit is proposed, which depends on the expected level of rotation/displacement ductility, wall geometry, reinforcement ratio and material properties.

2. Theory and formulation

2.1. Seismic behaviour

The behaviour of a reinforced concrete (RC) structure in an earthquake can significantly depart from its elastic behaviour due to cracking, tension stiffening, yielding of reinforcement and the nonlinear behaviour of concrete in compression. For example, the global nonlinear response of a typical reinforced concrete wall to an imposed lateral load/displacement is depicted in Figure 1. The reference coordinate system is commonly considered as the base shear vs. target lateral displacement (e.g. roof displacement), or the spectral acceleration vs. spectral displacement response spectrum (ADRS). The first notable point is the onset of cracking (Point C) at a critical location, e.g. the wall base in regular flexural structural walls (i.e. $H_w/L_w > 2$). Following this, reinforced concrete displays tension stiffening behaviour, and the capacity curve continues up to the first yield point (Point Yi). This corresponds to the formation of the first plastic hinge at the critical location, beyond which significant reductions in overall stiffness, and the inelastic dissipation of energy through plastic deformations, are expected. The capacity curve continues with the formation of consecutive plastic hinges at other potential locations, with a significant increase in the lateral displacement and a further increase in the force capacity. This commonly referred to as flexural overstrength, which is due to various factors such as the increased characteristic material strengths over design values, the inherent redundancy in the system and the strain hardening of steel reinforcement. This nonlinear behaviour continues up to the peak point (Point U), beyond which significant reduction in the overall force capacity is expected due to predominant softening behaviour at the critical locations and the influence of second-order effects.
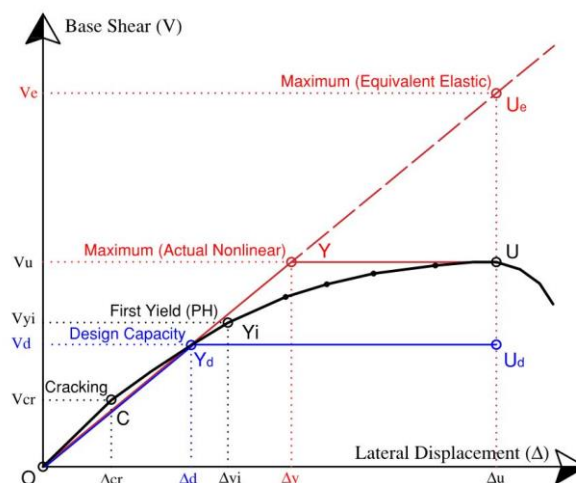

Figure 1. Schematic representation of the nonlinear response of reinforced concrete walls

The actual performance point of the structure in a design earthquake event is defined as the intersection between the earthquake demand spectrum and the expected capacity curve for the required performance level (typically Life Safety - LS). As this procedure is an iterative process, some standards, e.g. FEMA 440 (Federal Emergency Management Agency 2005) have proposed design equations for

predicting the expected target displacement (Δ_t), with the acceptable upper limit being the drift at ultimate capacity (Δ_u). For illustration purposes, we may assume the target performance point to coincide with the peak point on the capacity curve, although it is usually reserved for the maximum considered earthquake (MCE) with a higher return period, and for which the collapse prevention (CP) performance level is considered. As can be seen, the maximum level of lateral force (V_u) to be experienced in the design earthquake would be significantly less than that from the elastic response (V_e), which forms the basis for the definition of the structural ductility factor (μ_Δ) in the context of AS1170.4 (Standards Australia 2007) as:

$$\mu_\Delta = \Delta_u \big/ \Delta_y = V_e \big/ V_u \,. \tag{1}$$

The other essential parameters are denoted as follows:

$$S_p = V_d \big/ V_y = \Delta_d \big/ \Delta_y \,, \tag{2}$$

$$R = V_e \big/ V_d = \mu_\Delta \big/ S_p \,, \tag{3}$$

where S_p is the structural performance factor as the reciprocal of the structural overstrength factor ($\Omega = S_p^{-1}$), and R is the response modification factor for forced-based design using linear elastic analysis. In lieu of more rigorous pushover analysis, AS1170.4 and AS3600-2018 have suggested values for S_p and μ_Δ depending on the expected ductility level of the type of structure, assuming that an adequate level of seismic detailing is provided. It is also noted that in a forced-based design approach, special considerations must be made for the design of non-ductile actions and components. This includes an allowance for flexural overstrength and the consideration of the actual inelastic displacement, which has been commonly considered as the elastic displacement multiplied by the displacement amplification factor (C_d). Based on some simplified assumptions such as 5% overall damping in the design earthquake, AS1170.4 simply assumes the C_d factor to be identical to the response modification factor (R), i.e. $C_d = R = \mu_\Delta / S_p$.

As far as RC structural walls are concerned, a simple representation of how ductility is usually developed in the critical regions of flexural walls is illustrated in Figure 2. By increasing the lateral displacement, there will be a stage at which the critical section, which may be simply identified as the section with the highest demand to capacity ratio (DCR), reaches its yield capacity (M_y) and forms a plastic hinge (PH). The plastic rotation (θ_p) and the resulting idealised rigid body movement (Δ_p) of the wall are the main contributors to the displacement ductility and the dissipation of seismic energy. The critical region can potentially act as a "fuse" in the structural system, in a sense limiting the maximum level of seismic force experienced by the superstructure. The main concern is ensuring the uninterrupted development of ductility in the critical regions. This requires adequate level of detailing of the wall to ensure the stability of the BE as an idealised compression flange, and distributed cracking in the critical tension region as an idealised tension flange. In addition, it is necessary to prevent premature failure in brittle modes (e.g. shear failure), and to ensure that non-ductile elements have adequate drift capacity. In the context of this study, this means that if the compressive integrity of the BE is expected to be compromised due to the high level of curvature expected at a PH region, transverse reinforcement must be provided to effectively restrain critical compressive reinforcement against buckling, as well as provide an adequate level of confinement to the concrete core.

The yield displacement (Δ_y) can be expressed in terms of the associated yield curvature (φ_y) as follows:

$$\Delta_y = \varphi_y H^2 / \xi_y, \tag{4}$$

where the factor ξ_y is established from the basics of elastic structural mechanics depending on the distribution of equivalent lateral forces. This yields $\xi_y=3$ for an idealised point load applied at the top of the wall, and $\xi_y=40/11$ for a triangularly varying distributed load. Following this, the ultimate displacement of the wall (Δ_u) at the target location/height (H_t) can be established according to Figure 2 as:

$$\Delta_u = \Delta_y + (\varphi_u - \varphi_y) L_p (H_t - L_p/2), \tag{5}$$

for which the curvature values at yield and ultimate states will be later quantified in Sections 2.2 and 2.3, respectively. Moreover, L_p is the assumed length of the plastic hinge region, which has been quantified in various research studies (NEHRP Consultants 2014; Priestley et al. 2007) from which $L_p=0.5L_w$ and $L_p=0.2L_w+0.044H_w$ are two of the most commonly-used expressions. The former is the basis of ACI318 (American Concrete Institute 2019) and the latter is proposed in (Paulay and Priestley 1993), which is the underlying assumption in NZS3101 (New Zealand Standard 2006), and can be considered as the approximation of a more detailed equation proposed in (Priestley et al. 2007).
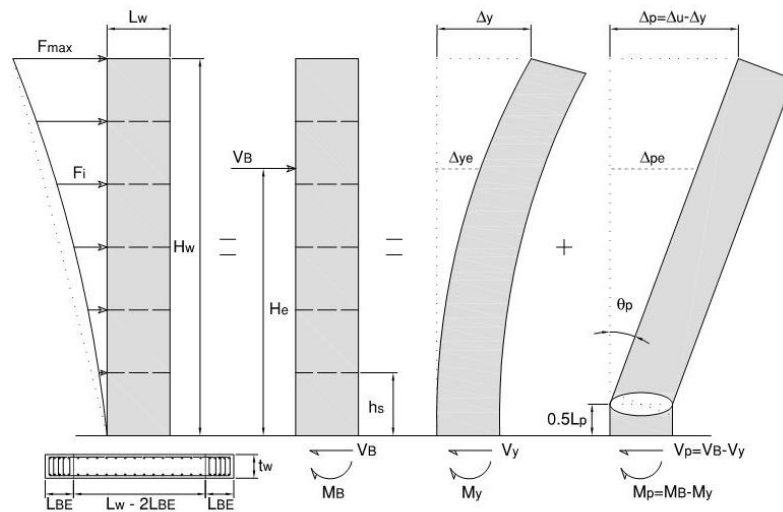

Figure 2. Simplified representation of ductility development in cantilevered structural walls.

In essence, equation (5) forms the basis of this study for evaluating the displacement ductility factor (μ_Δ) as the ratio of ultimate displacement with respect to equivalent yield displacement, i.e. reflected in equation (1). It is also noted that the reference location/height (H_t) for drift has been assumed to be either the total height (H_w), i.e. the roof displacement, or the effective height (H_e) of the structure based on the displacement of an equivalent single-degree-of-freedom system (SDOF), which can be evaluated from:

$$\Delta_e = \sum_{i=1}^{n} m_i \Delta_i^2 \Big/ \sum_{i=1}^{n} m_i \Delta_i, \tag{6}$$

in which m_i and Δ_i are the storey mass and lateral displacement, respectively. The effective height and displacement can be analytically established for different ductility levels from equations (1), (4)-(6), for which the effective height is commonly taken as $H_e=0.7H_w$ for ductile structures (Priestley et al. 2007).

2.2. Yield state

The state of yielding in a rectangular reinforced concrete wall section is schematically shown in Figure 3 in terms of the stress and strain distribution within the cross-section, where $d=\eta L_w$ is the effective yield depth and denotes the extent of the wall beyond which the steel reinforcement is expected to yield in tension.
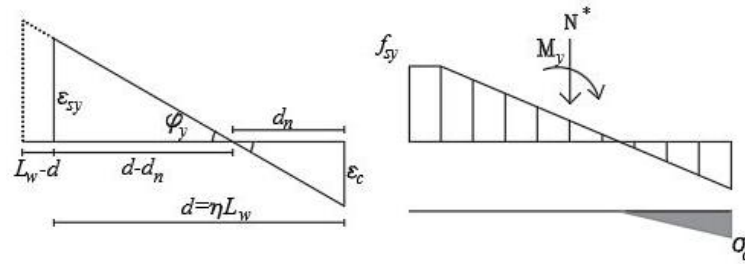

Figure 3. Idealised strain and stress distribution at the yield state.

By considering the strain compatibility within the section based on the assumption of linear strain distribution, the following quadratic equation can be established from the equilibrium equation of axial force as:

$$k_y{}^2 + \frac{2\rho_s n_s}{\eta}\left(\frac{\alpha_0}{m_s}+1\right)k_y - \frac{2\rho_s n_s}{\eta}\left(\frac{\alpha_0}{m_s}+1-\frac{\eta}{2}\right)=0 \quad \forall\, 0 \leq k_y \leq 0.5\eta, \qquad (7)$$

where $\rho_s=A_s/A_c$ is the steel reinforcement ratio, $n_s=E_s/E_c$ is the elastic modular ratio, $m_s=\rho_s f_{sy}/f'_c$ is the plastic mechanical reinforcement ratio, and $\alpha_0=N_0/(f'_c A_w)$ is the axial load ratio of the wall. The elastic mechanical reinforcement ratio may be expressed as $m_e=\rho_s n_s$ to simplify the governing equation (7), which yields the neutral axis depth ratio at the yield state ($k_y=d_{ny}/d$) as:

$$k_y = -\frac{m_e}{\eta}\left(\frac{\alpha_0}{m_s}+1\right)+\sqrt{\frac{m_e}{\eta}\left[\frac{m_e}{\eta}\left(\frac{\alpha_0}{m_s}+1\right)^2+\left(\frac{\alpha_0}{m_s}+1-\frac{\eta}{2}\right)\right]}. \qquad (8)$$

The curvature at first yield (φ_{yi}) corresponds to the yielding of the outermost layer of steel reinforcement and can be approximated by setting $\eta=1$. In contrast, the idealised yield curvature (φ_y), corresponding to the yield point on the equivalent bi-linear capacity curve, represents the state under which a fraction of the wall reinforcement has yielded, i.e. $\eta<1$. It is used as an index for evaluating the ductility in terms of displacement ($\mu_\Delta=\Delta_u/\Delta_y$) and/or curvature ($\mu_\varphi=\varphi_u/\varphi_y$). It has been commonly approximated as an amplification of the first-yield curvature:

$$\varphi_y = \Omega_y \varphi_{yi}, \text{ where } \varphi_{yi} = \frac{\varepsilon_{sy}}{\left(1-k_{yi}\right)L_w}. \qquad (9)$$

The overstrength factor for effective yield (Ω_y) is equal to V_y/V_{yi} or Δ_y/Δ_{yi}, and it has been suggested as 1.3 in NZS3101. By assuming C50 grade concrete with E_c=34.8 GPa according to AS3600-2018, and N500 grade steel reinforcement at a minimum percentage ($\rho_{s.min}$) to match the upper bound tensile capacity of concrete for distributed cracking of ρ_s=0.7$\sqrt{f'_c}/f_{sy}$≈1%, the neutral axis depth ratio at first yield is determined as k_{yi}=0.32 for a moderate axial load ratio (α_0=0.1). The effective yield curvature can thus be estimated as φ_y≈$1.3\varphi_{yi}$=$1.9\varepsilon_{sy}/L_w$, which is close to the commonly-used value of $2\varepsilon_{sy}/L_w$ proposed in (Priestley et al. 2007) for RC wall sections. The yield moment capacity (M_y) can be established from equilibrium and it is normalised against a reference elastic bending moment based on gross cross-section properties, M_c=$f'_c t_w L^2_w/6$, with the extreme fibre stress equal to f'_c, which yields:

$$M_y / M_c = m_s \left(1+1/m_e\right)\frac{3-2k_y}{\eta-k_y}k_y^2 - m_s\left[k_y^2 + k_y\left(\eta+1.5\right)+\eta\left(\eta-1.5\right)\right], \quad (10)$$

2.3. Ultimate state

The ultimate limit state (ULS) of a rectangular RC wall, in terms of the stress and strain distribution within the cross-section, schematically shown in Figure 4, is governed by the concrete crushing in compression.
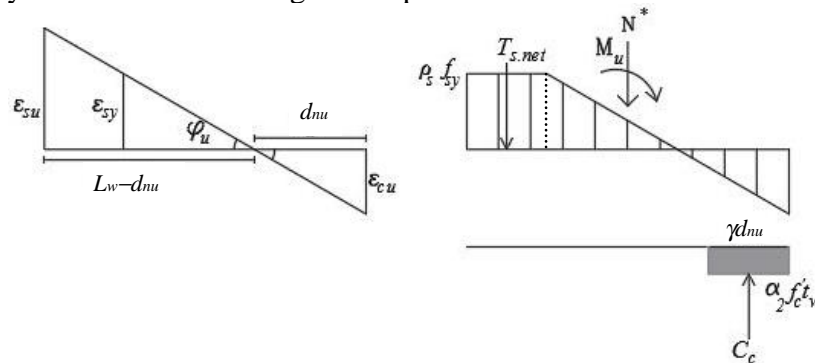

Figure 4. Idealised strain and stress distribution at the ultimate state.

The following two limits generally define the maximum compression fibre strain (ε_{cu}) that can be experienced at ULS in a section without the provision of transverse reinforcement:

A. The maximum compressive strain ($\varepsilon_{sc.lim}$) in the outermost layer of steel reinforcement beyond which the buckling of steel reinforcement and edge instability can potentially occur. This limit depends not only on the maximum compressive strain in a given compressive loading cycle, but also the maximum tensile strain (ε_{su}) that the steel experienced in its previous/reversal cycle in tension, which in turn governs the crack spacing and crack width. The influence of tensile cracking on maximum permissible compressive strain arises from the fact that each crack, while open, reduces the effective out-of-plane flexural stiffness of the wall to resist compression buckling due to loss of concrete contact. This limit has been defined implicitly or explicitly in the international design standards, e.g. 0.003 in (American Concrete Institute 2019; Canadian Standards Association 2004; Standards Australia 2018) or 0.0035 in (British Standards 2004; fib 2013; New Zealand Standard 2006).
B. The critical maximum compression fibre strain ($\varepsilon_{cu.lim}$) is the limit beyond which significant crushing is expected. Beyond this point, transverse reinforcement would be required to provide an adequate level of confinement to the concrete

core in order to safely reach the level of compressive strains expected in the plastic hinge regions. This limit has been recommended in ASCE41 (American Society of Civil Engineers 2017) as 0.002 in sections under predominant compression (i.e. compression-controlled behaviour), and it can be substantially higher up to 0.005 in sections under bending (i.e. tension-controlled behaviour).

By considering the idealised linear strain distribution within the cross-section, the following expression is obtained for the neutral axis depth ratio at ULS (k_u) from the equilibrium between internal and external forces on the section:

$$k_u = \left(\alpha_2 \gamma + 2 m_s\right)\big/\left(\alpha_0 + m_s\right) \quad \forall \; 0 \le k_u \le 0.5, \tag{11}$$

where α_2 and γ are the parameters of the equivalent rectangular stress block corresponding to the strain state. By assuming $\varepsilon_{cu}=0.003$, the maximum allowable axial load ratio limit ($\alpha_0 \le \alpha_{0.max}$) can be evaluated for a given depth of neutral axis as a measure of ductility. On this basis, the maximum axial load ratio for C50 walls are listed in Table 1 for different mechanical reinforcement ratios and neutral axis depth ratios. Beyond these limits, transverse reinforcement is required in the BE to allow safe exceedance of the maximum compression strain. Thereby, despite AS3600-2018 prescribing the maximum axial stress of 0.2f'$_c$ for walls with $\mu_\Delta>1$, more stringent limits may apply if confined boundary elements are to be avoided.

Table 1. Maximum axial load ratio ($\alpha_{0.max}$) in walls without confined boundary elements

k_u	m_s			
	0.05	0.1	0.15	0.20
0.075	0.00	BE req.	BE req.	BE req.
0.130	0.04	0.00	BE req.	BE req.
0.170	0.07	0.04	0.00	BE req.
0.205	0.09	0.06	0.03	0.00
0.250	0.12	0.10	0.07	0.05
0.300	0.16	0.14	0.12	0.10
0.375	0.21	0.20	0.19	0.17

By applying algebraic manipulations on equation (5), the ultimate curvature can be expressed in terms of the target level of ultimate drift ($d_u=\Delta_u/H_w$) as:

$$\varphi_u = \frac{\varepsilon_{cu}}{k_u L_w} = \frac{\xi_y\left(r_p/r_w\right)\left(1-0.5\,r_p/r_w\right)+\mu_\Delta-1}{\mu_\Delta H_w\left(r_p/r_w\right)\left(1-0.5\,r_p/r_w\right)}\left(\frac{\Delta_u}{H_w}\right), \tag{12}$$

where $r_w=H_w/L_w$ and $r_p=L_p/L_w$ are the aspect ratios of the wall and its PH, respectively. Equation (12) can also be rearranged to represent the neutral axis depth ratio in terms of the ultimate drift. Since the yield curvature can be expressed as $\varphi_y=\xi_y\times(\Delta_u/H_w)/(\mu_\Delta H_w)$, the following expression is obtained from equation (12) for the curvature/rotation ductility:

$$\mu_\varphi = \frac{\mu_\Delta-1}{\xi_y\left(r_p/r_w\right)\left(1-0.5\,r_p/r_w\right)}+1, \tag{13}$$

This yields one of the commonly used approximations of curvature ductility as $\mu_\varphi = 2\mu_\Delta - 1$ in Eurocode 8 if the denominator tends to 0.5, which would require $H_w/L_p \approx 7$. Using the same normalisation against the reference elastic moment as in equation (10), the ultimate bending moment capacity of the section (M_u) can be also found from the equilibrium condition as:

$$M_u/M_c = \left[3\alpha_2\gamma(\gamma+2)+4m_s\right]k_u^2 + 3\left(\alpha_2\gamma - 2\alpha_0\right)k_u. \tag{14}$$

The strain-based methods (Wallace 1995, 2012; Wallace and Orakcal 2002) for the requirement of BE are generally expressed in terms of either a minimum limit for the ultimate curvature ($\varphi_u \geq \varphi_{u.lim}$), or more commonly as a maximum limit for the neutral axis depth ratio ($k_u \leq k_{u.lim}$). To establish a conceptual link between strain-based methods and an equivalent elastic stress-state based on gross-section behaviour, the maximum allowable demand moment (M^*_{max}) in conventional force-based design per Figure 1 is assumed to be equal to the factored bending moment capacity (ϕM_u). This equivalent linear elastic stress state is schematically illustrated in Figure 5 and along with the axial load ratio, results in the following expression for the maximum fibre stress index in compression:

$$\beta = \sigma_{ce.max}\Big/ f_c' = \alpha_0 + \phi M_u / M_c, \tag{15}$$

Note that the stress limit obtained from equation (15) is merely an index value for the requirement of confined boundary elements, and the associated linear elastic stress state as shown in Figure 5 does not represent the actual stress state at ULS per Figure 4. The equivalent yield state on the idealised bi-linear capacity curve, see Figure 1, is assumed in the context of AS1170.4 and AS3600 to be equal to the unfactored ultimate capacity of the section based on characteristic strength values, and without consideration of strain hardening of steel reinforcement. On this basis, the dimensionless effective depth (η) and the neutral axis depth ratio (k_y) of the section at the equivalent yield state can be calculated by equating M_y from equation (10) with M_u in an iterative approach. This in return results in the following expressions for the equivalent yield curvature (φ_y) and the overstrength factor for effective yield (Ω_y):

$$\varphi_y = \frac{\varepsilon_{sy}}{\left(\eta-k_y\right)L_w} \text{ and } \Omega_y = \frac{1-k_{yi}}{\eta-k_y}. \tag{16}$$
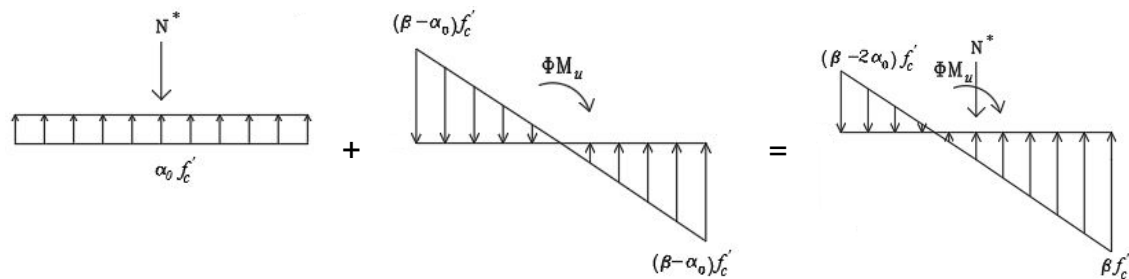

Figure 5. Conceptual illustration of the proposed linear elastic stress-based method.

3. Results and discussion

In this section, some indicative results from the proposed method are presented and discussed. In the following examples, an individual reinforced concrete wall section, with dimensions set at L_w=5 m and t_w=0.2 m, is considered with various aspect ratios

and percentages of steel reinforcement, and subject to a triangular distributed load as an idealised load pattern for a design seismic event. The concrete grade and the reinforcement class are assumed to be C50 and N500, respectively. These assumptions can be easily adjusted for other parameters in future studies. The assumed thickness is chosen as the minimum based on the slenderness limits in AS3600-2018 for LDW and MDW which are 20 and 16, respectively, and a storey height (i.e. h_s=3.1 m), fairly typical of Australian residential building practice.

In the first example, the performance of the proposed method is compared with one of the pioneering strain-based methods (Wallace 1995), which shares a similar framework with this study except for a simplified assumption for curvature. Wallace et al. (Wallace 1995) assumed the depth of neutral axis at the yield and ultimate states to be equal and irrespective of the steel reinforcement ratio, i.e. d_{ny}=d_{nu} or μ_φ=($\varepsilon_{cu}/\varepsilon_{sy}$)×(1-$k_u$)/$k_u$. A comparison with the strain-based method in ACI318 is also included, which can be considered as the simplified version of the Wallace method by approximating the ultimate lateral displacement in equation (5) with $\Delta_u \approx \varphi_u L_p H_w$. A SDW ($\mu_\Delta$=4) has been considered in this introductory example with a peak compressive strain of ε_{cu}=0.003, and the results are shown in Figure 6 for various mechanical reinforcement ratios as per (a) the strain-based approach according to equation (12) in terms of critical neutral axis depth ratio ($k_{u.lim}$), and (b) the consistent stress-based approach according to equation (15) in terms of the extreme compressive fibre stress index (β_{lim}) based on linear elastic analysis and gross section properties. In both graphs, the region above the relevant criteria curve corresponds to the requirement of boundary elements. As can be seen, the proposed solution is in good agreement with the Wallace and the ACI318 methods. In addition, it accounts for the impact of the reinforcement ratio.
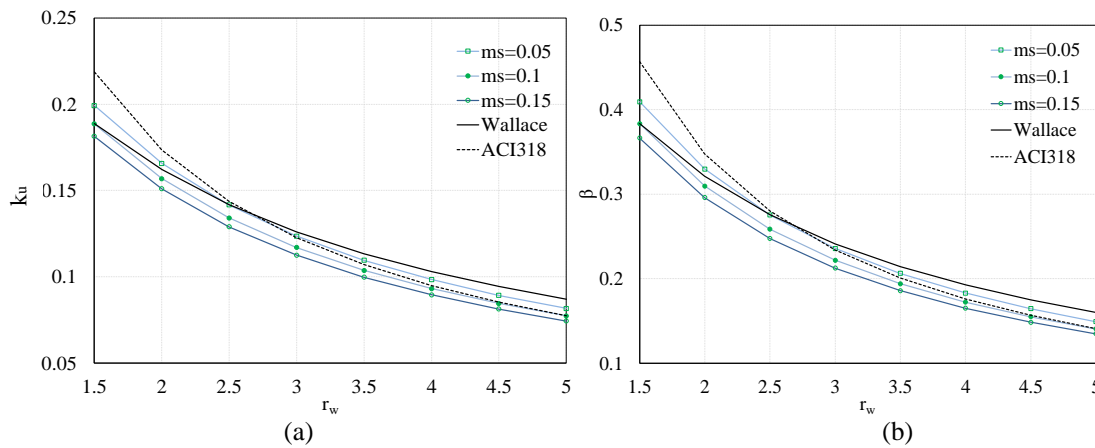

Figure 6. Comparison between the boundary element requirement criterion in ductile walls at different aspect ratios based on: (a) The strain-based method expressed in terms of k_u, (b) The consistent stress-based method expressed in terms of β.

Following this initial comparison, the limits for the requirement of BE are studied more extensively by the inclusion of low (μ_Δ=2) and moderate (μ_Δ=3) ductility classes. The criteria curves in both approaches, strain-based and stress-based, are shown in Figure 7 and Figure 8 for walls with negligible ($\alpha_0 \approx 0$) and low (α_0=0.05) axial load ratio, respectively. The dashed portions of the lines conservatively indicate where the peak compression strain would need to exceed the limits beyond which BE are required, in order to satisfy equilibrium as per equation (11) for the level of axial load defined by α_0.
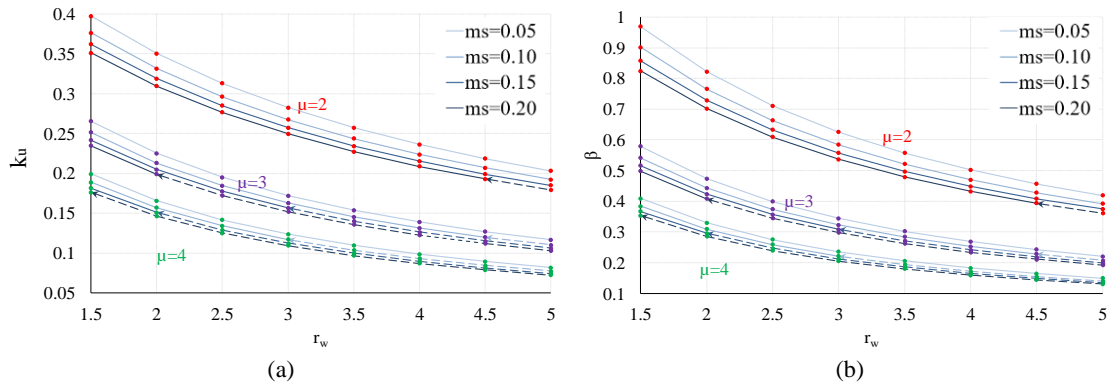
(a)

(b)

Figure 7. The criteria for requiring confined boundary elements in walls with no axial load (α_0=0), and different ductility classes (μ_Δ), as a function of aspect ratio (r_w) and mechanical reinforcement ratio (m_s) based on: (a) strain-based limit in terms of k_u, (b) consistent linear elastic stress-based limit in terms of β.

(a)

(b)
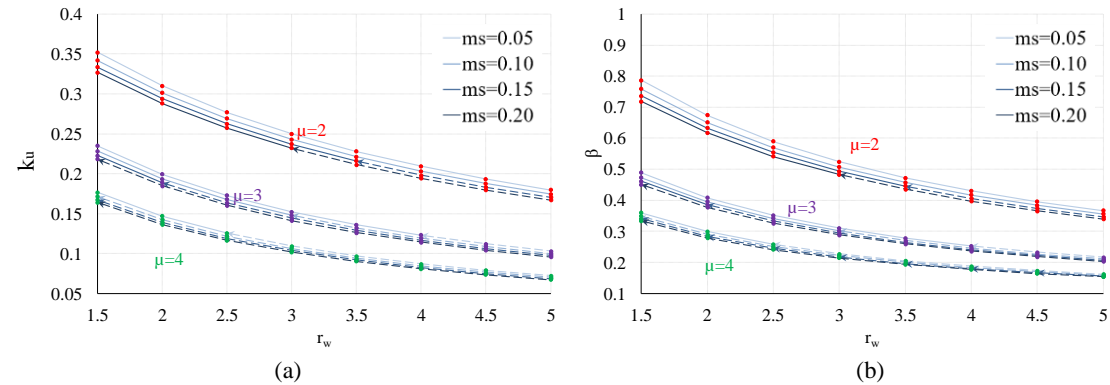
Figure 8. The criteria for requiring confined boundary elements in walls with low axial load (α_0=0.05), and different ductility classes (μ_Δ), as a function of aspect ratio (r_w) and mechanical reinforcement ratio (m_s) based on: (a) strain-based limit in terms of k_u, (b) consistent linear elastic stress-based limit in terms of β.

Figure 7 and Figure 8 show the maximum limits for the neutral axis depth ratio ($k_u \le k_{u.lim}$) and the equivalent extreme fibre compression stress parameter ($\beta \le \beta_{lim}$) for avoiding the need to provide BE. These limits can be seen to reduce with increased ductility, reinforcement ratio and axial load. For a moderate aspect ratio of r_w=3.5, the critical neutral axis depth ratio ($k_{u.lim}$) is approximately 0.1 in SDW (μ_Δ=4), which matches closely with the requirements of ACI318 for an ultimate drift of 1.5%. It is 0.15 for MDW, which is consistent with the requirements in NZS3101, and 0.24 for LDW. The consistent stress limit index (β_{lim}) also follows a similar pattern and is approximately 0.2, which is consistent with the stress-based method in ACI318 for SDW. It is approximately 0.3 for MDW, and is approximately 0.5 for LDW, however the latter is not expected to be exceeded in the majority of practical design scenarios. The effects of varying the reinforcement ratio also follow the same trends between the strain-based and stress-based methods as can be seen in the figures. This highlights the conservatism and inconsistency of a single critical value for the extreme fibre compressive stress of 0.15f'$_c$ in AS3600 for the requirement of BE for LDW and MDW. The limit of 0.15f'$_c$ (β_{lim}=0.15) appears to be an especially conservative value for LDW, and as can be seen from Figure 7 and Figure 8, it is more stringent than required for MDW (μ_Δ=3), and most cases of SDW (μ_Δ=4) over the range of aspect ratio assessed. Furthermore, β_{lim} shows a clear dependence on the ductility level (μ_Δ), which demonstrates the unsuitability of an identical limit in AS3600-2018 for LDW and MDW. As the seismic load case used to assess the extreme fibre compressive stress is reduced by the response modification factor ($R=\mu/S_p$), this can result in less BE in MDW than LDW, or none at all. This is counterintuitive and goes against the intent of ductile detailing.

Since the requirement of BE appears to show a strong dependence on the influence of the axial load level, especially in walls with low ductility, the sensitivity of this parameter was studied. A moderate level of vertical reinforcement was considered (i.e. m_s=0.15), and the results are presented in Figure 9 for LDW systems. As can be seen, the thresholds of both the stress limit index (β_{lim}) and the critical neutral axis depth ratio ($k_{u.lim}$), before BE are required, decrease significantly in response to increases in the axial load level. Furthermore, the acceptable range of combinations of β_{lim} and $k_{u.lim}$ with r_w, as highlighted by solid lines, also shrinks with increased axial load level on the walls. This indicates a limited range of possible aspect ratios ($r_w \leq 2.5$) for α_0=0.1 and almost none for $\alpha_0 \geq 0.15$.
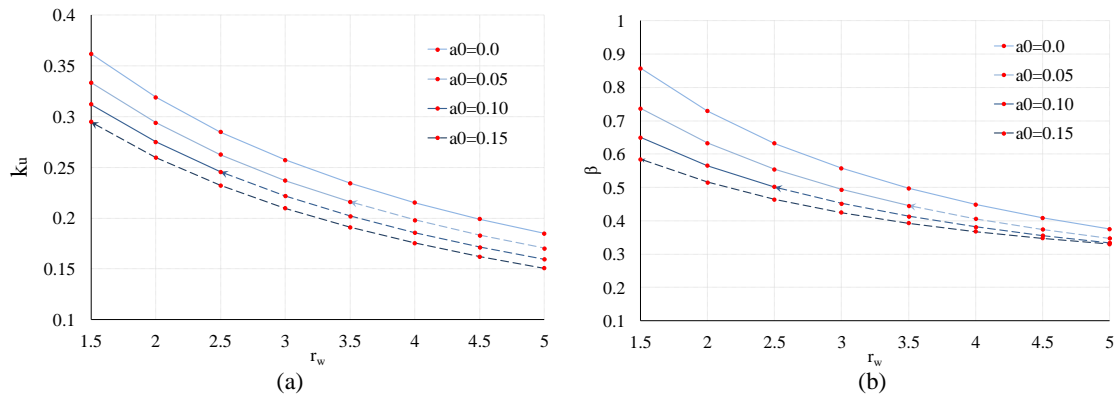

Figure 9. The criteria for requiring confined boundary elements in limited ductile walls (μ_Δ=2) with a moderate level of mechanical reinforcement ratio (m_s=0.15) as a function of aspect ratio (r_w) and axial load ratio (α_0), based on: (a) strain-based limit in terms of k_u, (b) consistent linear elastic stress-based limit in terms of β.

An additional parametric study was performed on different ductility classes with reference to the ultimate drift, rather than the overall aspect ratio. The aspect ratio (r_w) was set as 2, with α_0=0. The critical ultimate curvature ($\varphi_{u.lim}$) and the neutral axis depth ratio ($k_{u.lim}$) can be calculated from equation (12) for a target level of ultimate drift (d_u), which can be then transformed into an equivalent linear elastic stress limit (β_{lim}) by equation (15). The criteria curves for the requirement of confined boundary elements are shown in Figure 10 based on $\varepsilon_{cu.lim}$=0.003. The minor differences in the overlapping portions of the lines between different ductility classes are due to the dependence of ultimate curvature on the ductility factor (μ_Δ), as per Equation (12). However, the differences would be more pronounced if a different limit for the critical compression strain was used for each ductility class. This is based on the requirement of lateral restraint of critical compressive reinforcement against buckling under low cycle fatigue as per section 2.3.A, and as such the critical total reinforcement strain $\varepsilon_{sm}=\varepsilon_{su}+\varepsilon_{cu}$ may be a more realistic limit. This could be a subject for further study, however, the limit for ε_{cu} as per section 2.3.B regarding confinement to the concrete core still needs to be adhered to.
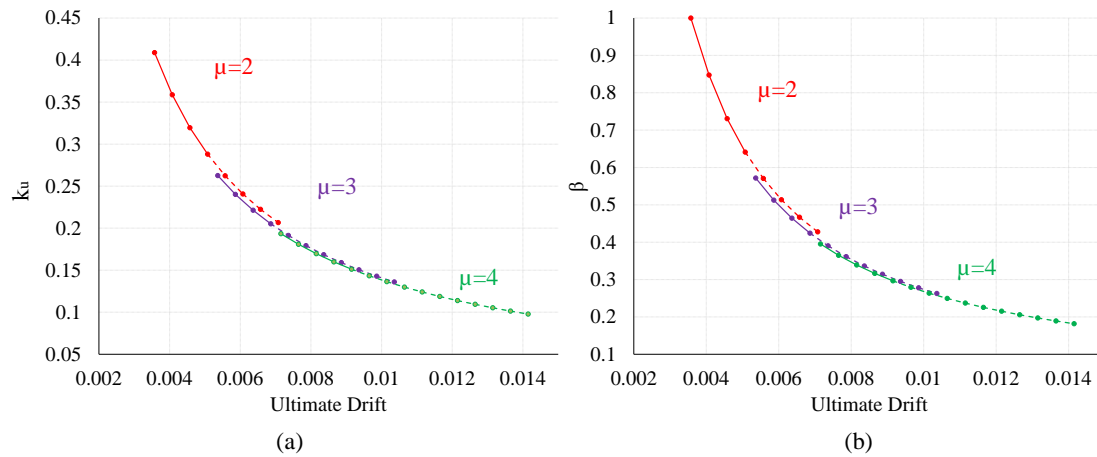
Figure 10. The Criteria for requiring confined boundary elements in walls no axial load ($\alpha_0=0$) and different ductility classes (μ_Δ) at various ultimate drift levels, based on (a) strain-based limit in terms of k_u, (b) consistent linear elastic stress-based limit in terms of β.

The curve for each ductility class in Figure 10 has been plotted with each point representing a different reinforcement ratio (m_s). The drift interval is thus defined by the minimum yield curvature with low m_s, and the maximum drift is obtained from the yield state but with the maximum limit on the depth of neutral axis consistent with the peak compression strain for the onset of crushing. Similar to Figure 7 and Figure 8, the solid line becoming dashed also indicates the maximum drift limit for each ductility class beyond which confined boundary elements are required so that the peak strain can exceed the critical level in order to satisfy equilibrium. One possible interpretation of the figures for designers is the practical range of drift for each ductility class and the level of drift limit beyond which switching to a higher ductility class may enable BE to be avoided. High-strength concrete walls are another major shortcoming of conventional stress-based methods to assess the requirement of boundary elements, as the limiting stress increases with f'$_c$, and does not account for the increased brittleness over and above normal strength concrete. The proposed method partially addresses this by being established from rational strain-based assessment, while accounting for the brittleness of high-strength concrete in compression block properties. Further consideration can also be given by penalising the maximum compressive strain to a lower limit for high-strength concrete, e.g. 0.0025.

4. Conclusions

A consistent stress-based criterion for the requirement of confined boundary elements in walls with low to moderate ductility is proposed in this paper, and was established theoretically upon a rational strain-based assessment. The proposed method addresses some of the shortcomings of the conventional stress-based criteria, such as in AS3600-2018, while retaining its ease of implementation by practitioners in comparison with more complicated and rigorous strain-based methods. The following conclusions are drawn from the theory and the results of this study:

- The single-limit stress-based criterion in AS3600-2018 is conservative and inconsistent in terms of the expected level of ductility from moderately ductile and especially limited ductile structural walls;
- The proposed adjustable stress limit is comprehensive by considering the expected level of ductility, wall geometry, and material properties; and

- The proposed stress-based criterion is shown not only to be in good agreement with well-known strain-based methods incorporated in other international design standards, but also to properly account for the effects of the reinforcement ratio and concrete grade.

5. References

American Concrete Institute. (2019). *ACI 318-19 Building Code Requirements for Structural Concrete*.

American Society of Civil Engineers. (2017). *ASCE/SEI 41 Seismic Evaluation and Retrofit of Existing Buildings*.

British Standards. (2004). *BS EN 1998-1 Eurocode 8: Design of structures for earthquake resistance*.

Canadian Standards Association. (2004). *CSA A23.3 Design of concrete structures*.

Federal Emergency Management Agency. (2005). *FEMA 440 Improvement of Nonlinear Static Seismic Analysis Procedures*.

fib. (2013). *fib Model Code for Concrete Structures 2010*.

Menegon, S. J. (2018). "Displacement Behaviour of Reinforced Concrete Walls in Regions of Lower Seismicity." Swinburne University of Technology.

Menegon, S. J., Wilson, J. L., Lam, N. T. K. K., and McBean, P. (2018). "RC walls in Australia: seismic design and detailing to AS 1170.4 and AS 3600." *Australian Journal of Structural Engineering*, Taylor & Francis, 19(1), 67–84.

NEHRP Consultants. (2014). *NIST GCR 14-917-25, Recommendations for Seismic Design of Reinforced Concrete Wall Buildings Based on Studies of the 2010 Maule, Chile Earthquake*.

New Zealand Standard. (2006). *NZS 3101.1:2006 Concrete structures standard*.

Paulay, T., and Priestley, M. J. N. (1993). "Stability of Ductile Structural Walls." *ACI Structural Journal*, 90(4).

Priestley, M. J. N., Calvi, G. M., and Kowalsky, M. J. (2007). *Displacement-based seismic design of structures*. IUSS Press.

Standards Australia. (2007). *AS 1170.4 Structural Design Actions, Part 4: Earthquake actions in Australia*.

Standards Australia. (2009). *Concrete structures. AS3600: 2009*. Standards Australia.

Standards Australia. (2018). *AS 3600-2018 Concrete Structures*.

Wallace, J. W. (1995). "Seismic Design of RC Structural Walls. Part I: New Code Format." *Journal of Structural Engineering*, 121(1), 75–87.

Wallace, J. W. (2012). "Behavior, design, and modeling of structural walls and coupling beams — Lessons from recent laboratory tests and earthquakes." *International Journal of Concrete Structures and Materials*, 6(1), 3–18.

Wallace, J. W., and Moehle, J. P. (1992). "Ductility and Detailing Requirements of Bearing Wall Buildings." *Journal of Structural Engineering*, 118(6), 1625–1644.

Wallace, J. W., and Orakcal, K. (2002). "ACI 318-99 Provisions for Seismic Design of Structural Walls." *ACI Structural Journal*, 99(4), 499–508.